Scaling and universality in the aging kinetics of the two-dimensional clock model

Federico Corberi,* Eugenio Lippiello,† and Marco Zannetti‡
Istituto Nazionale di Fisica della Materia, Unità di Salerno and Dipartimento di Fisica "E.Caianiello," Università di Salerno, 84081 Baronissi (Salerno), Italy

(Received 2 November 2005; revised manuscript received 4 July 2006; published 6 October 2006)

We study numerically the aging dynamics of the two-dimensional p-state clock model after a quench from an infinite temperature to the ferromagnetic phase or to the Kosterlitz-Thouless phase. The system exhibits the general scaling behavior characteristic of nondisordered coarsening systems. For quenches to the ferromagnetic phase, the value of the dynamical exponents suggests that the model belongs to the Ising-type universality class. Specifically, for the integrated response function $\chi(t,s) \simeq s^{-a_\chi} f(t/s)$, we find a_χ consistent with the value $a_\chi = 0.28$ found in the two-dimensional Ising model.

DOI: 10.1103/PhysRevE.74.041106 PACS number(s): 05.70.Ln, 75.40.Gb, 05.40.−a

I. INTRODUCTION

The phase-ordering kinetics of systems quenched from a high-temperature disordered state to an ordered phase or to a critical phase is characterized by the growth of a characteristic length $L(t)$. In the late stage a power-law behavior

$$L(t) \sim t^{1/z} \tag{1}$$

sets in, where z is the dynamical exponent, and dynamical scaling [1] is observed. Accordingly, configurations of the system at two subsequent times are statistically equivalent if lengths are measured in units of $L(t)$, namely if the rescaled length $x = r/L(t)$ is considered. This property is reflected by the analytical form of physical observables. In the quench to a critical point, for example, the equal-time order parameter correlation function obeys the scaling form

$$G(\vec{r},t) \sim r^{-(d-2+\eta)} g(x), \tag{2}$$

where d is the spatial dimensionality and η is the usual exponent of static critical phenomena. Scaling behaviors such as Eqs. (1), (2) are generic for growth kinetics in nonfrustrated, nondisordered systems and are observed regardless of different specific details. Concerning the values of the exponents, such as z or others entering different quantities, they are expected to take the same value for systems belonging to the same nonequilibrium universality class. It is well known that systems undergoing a second order equilibrium phase transition can be classified into static equilibrium universality classes according to the value of their critical indices. These are found to depend only on a small set of parameters, such as space dimensionality or the number of components of the order parameter. In the same way, dynamic universality classes can also be introduced on the basis of the value of dynamic exponents. This subject has been thoroughly studied for the equilibrium critical dynamics [2], where the renormalization group provides the basic mechanism for scaling and universality, analogously to the static case. By contrast, the same subject is not well understood in far from equilibrium systems [3,4].

In this paper we consider the phase-ordering kinetics of the clock model with a p-fold degenerate ground state in two dimensions. For $p \leq 4$ this model has a single second order phase transition separating a disordered from an ordered phase. For $p \geq 5$ a Kosterlitz-Thouless (KT) critical phase also exists and the phase transitions are of the Kosterlitz-Thouless type. We study numerically the model with $p=3$ and $p=6$ and a nonconserved order parameter, quenched to the ordered region and, for the case $p=6$, also to the KT phase. In previous works [5,6] the growth law (1) and the scaling of $G(\vec{r},t)$ in quenches to the ordered region were analyzed; for quenches to a critical point, two time quantities were studied in Ref. [3]. Here we extend these results presenting a global analysis of the scaling properties for quenches in the ordered and in the critical region, by considering one-time quantities, such as $G(\vec{r},t)$, and two-time quantities, such as the autocorrelation function and the integrated response function. We find that the scaling forms expected for all these quantities in nondisordered systems are obeyed, although preasymptotic corrections are observed in the simulated range of times. We may then conclude that the clock model exhibits the generic scaling behavior characteristic of phase-ordering systems in the late stage of the dynamics. This calls for the question of the value of the dynamical exponents and the issue of their universality, namely whether the dynamics of the model is regulated by the same exponents of other coarsening systems and whether their value depends on p. Since in the KT phase critical exponents depend continuously on temperature, this problem is pertinent to the quench to the ordered phase. Among the most usually considered two-dimensional statistical models of ferromagnetism, the Ising and the XY model are those to which the clock model can be naturally compared. These models are particular cases, with $p=2$ and $p=\infty$, of the clock model. The former has a scalar order parameter and a discrete symmetry. In the latter, the order parameter is a vector with $N=2$ components and there is a continuous $O(2)$ symmetry. The symmetry group of the model, together with the spatial dimensionality, determines the types of topological defects. Consequently, topological defects are interfaces or two-dimensional vortices in the Ising and XY model, respectively.

*Electronic address: corberi@na.infn.it
†Electronic address: lippiello@sa.infn.it
‡Electronic address: zannetti@na.infn.it

Since the nature of the topological defects controls several equilibrium properties and the late stage ordering [1] these models belong to different universality classes both in equilibrium and out of equilibrium. The clock model is, in some sense, intermediate between the Ising and *XY* model, because the order parameter is a vector with two components, as in the *XY* model, but there is a finite degeneracy of the ground state, namely a discrete symmetry. Topological defects are then both interfaces and vortices.

In this paper we show that the exponents measured for the phase-ordering kinetics of the clock model with $p=3$, 6 are consistent with those of the two-dimensional Ising model quenched below the critical temperature. This suggests that systems with a finite degeneracy of the ground state may belong to the Ising nonequilibrium universality class, and that the presence of other topological defects besides interfaces does not affect the universal properties of these systems.

This paper is organized as follows: In Sec. II we introduce the model and define the main observables. In Sec. III we discuss the general scaling behavior of systems quenched into an ordered region, present the results of numerical simulations of the clock model with $p=3$ and $p=6$, and compare them with the behavior of the Ising model and of the *XY* model. In Sec. IV we discuss the scaling properties of coarsening systems quenched to a critical phase and the results of numerical simulations of the clock model with $p=6$ quenched into the KT phase. Section V contains the final observations and the conclusions.

II. MODEL AND OBSERVABLES

The p-state clock model is defined by the Hamiltonian

$$H[\sigma] = -J\sum_{\langle ij\rangle} \vec{\sigma}_i \cdot \vec{\sigma}_j = -J\sum_{\langle ij\rangle} \cos(\theta_i - \theta_j), \tag{3}$$

where $\vec{\sigma}_i$ is a two-component unit vector spin pointing along one of the directions $\theta_i = 2\pi n_i/p$, with $n_i \in \{1,2,\ldots,p\}$, and $\langle ij\rangle$ denotes nearest neighbors sites i, j on a lattice. We will consider a square lattice in spatial dimension $d=2$. This spin system is equivalent to the Ising model for $p=2$ and to the *XY* model for $p\to\infty$.

For $p\leq 4$ the clock model has a critical point separating a disordered from an ordered phase at $T=T_1$. For $p\geq 5$ there exist two transition temperatures T_1 and $T_2 > T_1$ [7]. For $T < T_1$ the system is ferromagnetic, and for $T > T_2$ it is in a paramagnetic phase. Between these two temperatures, for $T_1 < T < T_2$, a KT phase [8] exists where the correlation function behaves as $G_{eq}(r) \sim |r|^{-\eta(T)}$ with the anomalous dimension $\eta(T)$ continuously depending on the temperature. Both the transitions are of the KT type, namely the correlation length diverges exponentially as T_1 or T_2 are approached from the ferromagnetic or paramagnetic phase, respectively. Approximate analytic results [7] predict

$$T_1/J = \frac{4\pi^2}{1.7p^2} \tag{4}$$

and T_2 to coincide with the KT temperature of the *XY* model $T_2/J = 0.95$ (here and in the following we set the Boltzmann constant $k_B=1$). The exponent $\eta(T)$ is expected [7] to vary between $\eta(T_1)=4/p^2$ and $\eta(T_2)=1/4$. Numerical simulations [9] are consistent with these predictions.

A dynamics is introduced by randomly choosing a single spin and updating it with Metropolis transition rate

$$w([\sigma]\to[\sigma']) = \min[1, \exp(-\Delta E/T)]. \tag{5}$$

Here $[\sigma]$ and $[\sigma']$ are the spin configurations before and after the move, and $\Delta E = H[\sigma'] - H[\sigma]$.

We consider the protocol where the system is initially prepared in a high temperature uncorrelated state and then quenched, at time $t=0$, to a final temperature T_f in the ferromagnetic phase or in the KT phase. The characteristic size $L(t)$ grows until it becomes comparable with the system size and the new equilibrium state at T_f is globally attained. For an infinite system the final equilibrium state is never reached and $L(t)$ keeps growing indefinitely. In the late stage the power law (1) sets in. The characteristic length $L(t)$ can be estimated from the knowledge of the two-point equal time correlation function

$$G(r,t) = \langle \vec{\sigma}_i(t) \cdot \vec{\sigma}_j(t)\rangle, \tag{6}$$

where $\vec{\sigma}_i(t)$, $\vec{\sigma}_j(t)$ are spin variables at time t on two lattice sites whose distance is r, and $\langle\cdots\rangle$ means an ensemble average, namely taken over different initial conditions and thermal histories. Due to homogeneity, $G(r,t)$ does not depend separately on i an j but only on r. Enforcing this property we will numerically compute the correlation in the following as

$$G(r,t) = \frac{1}{4N}\sum_i \sum_{j\in J_+} \langle \vec{\sigma}_i(t) \cdot \vec{\sigma}_j(t)\rangle, \tag{7}$$

where i runs over all the N sites of the lattice and J_+ is the set of four points reached moving a distance r from i along the horizontal or vertical directions. The methods to extract $L(t)$ from $G(r,t)$ depend on the scaling properties of $G(r,t)$ and differ if quenches in the ferromagnetic or in the KT phase are considered, as discussed in Secs. III and IV.

The two time quantities that will be considered in this paper are the autocorrelation function

$$C(t,s) = \langle \vec{\sigma}_i(t) \cdot \vec{\sigma}_i(s)\rangle \tag{8}$$

and the integrated (auto)response function, or zero field cooled susceptibility

$$\chi(t,s) = \int_s^t dt' R(t,t'). \tag{9}$$

The quantity

$$R(t,t') = \sum_\alpha \left.\frac{\partial\langle \sigma_i^\alpha(t)\rangle}{\partial h_i^\alpha(t')}\right|_{h=0}, \tag{10}$$

α being a generic vector component, is the response function associated to the perturbation caused by an impulsive magnetic field $\vec{h}_i$ switched on at time $t' < t$. Recently, new efficient methods for measuring the response function without applying the perturbation have been introduced [10–12]. In the following we will use the one derived in Ref. [12]. For

spin systems subjected to a Markovian dynamics an out of equilibrium generalization of the fluctuation dissipation theorem was derived [13], relating the response functions to particular correlation functions of the unperturbed system. For the integrated response function (9) it reads

$$T\chi(t,s) = \frac{1}{2}\left[C(t,t) - C(t,s) - \int_s^t \langle \vec{\sigma}_i(t) \cdot \vec{B}_i(t') \rangle dt' \right], \tag{11}$$

where

$$\vec{B}_i[\sigma] = -\sum_{\vec{\sigma}'} (\vec{\sigma}_i - \vec{\sigma}_i') w([\sigma] \to [\sigma']). \tag{12}$$

In this equation $[\sigma]$ and $[\sigma']$ are two configurations differing only by the spin on site i, taking the values $\vec{\sigma}_i$ and $\vec{\sigma}_i'$, respectively. The notation $\langle \vec{\sigma}_i(t) \cdot \vec{B}_i(t') \rangle$ in Eq. (11) means the average $\Sigma_{[\sigma],[\sigma']} \vec{\sigma}_i \cdot \vec{B}_i[\sigma'] p([\sigma],t;[\sigma'],t') p([\sigma'],t')$, where $p([\sigma'],t')$ is the probability to find the configuration $[\sigma']$ at time t' and $p([\sigma],t;[\sigma'],t')$ is the joint probability between $[\sigma]$ at time t and $[\sigma']$ at time t'.

Equation (11) allows us to compute the integrated response function by measuring correlation functions on the unperturbed system, avoiding the complications of the traditional methods where a perturbation is applied, and improving significantly the quality of the results [12].

III. QUENCHES TO $T_f < T_1$

A. General scaling properties

Let us start considering quenches from a high temperature disordered phase to the ferromagnetic region. In this case one observes the growth of compact domains separated by topological defects such as interfaces or vortices (see Fig. 2). As a consequence, a sharp distinction can be made in the late stage between spins belonging to the interior of domains from those pertaining to the defects. The interior of the domains very soon attains local equilibration in one of the broken symmetry equilibrium phases at T_f, whereas the degrees of freedom around defects are out of equilibrium and are responsible for the aging of the system. Observables such as $C(t,s)$, $\chi(t,s)$, and $G(r,t)$ take an addictive structure [14]

$$C(t,s) = C_{st}(t-s) + C_{ag}(t,s), \tag{13}$$

and similarly for $\chi(t,s)$ and $G(r,t)$. In the following, for clarity, we will focus on $C(t,s)$, but similar considerations hold for the other quantities. The dynamics of the spins in the bulk of domains provide the equilibrium contribution $C_{st}(t-s)$ while what is left over, $C_{ag}(t,s)$, accounts for the aging behavior. Since equilibrium dynamics is well understood, the behavior of $C_{st}(t-s)$ is generally well known. In particular, at $T_f=0$ equilibrium dynamics is frozen and $C_{st}(t-s) \equiv 0$. On the other hand, much interest is focused on the aging part of the aforementioned observables, which is less understood. This contribution can be isolated by subtracting $C_{st}(t-s)$, computed in equilibrium, from $C(t,s)$. However, for models with a discrete symmetry, it is computationally much more efficient to resort to a different method. This amounts to study a modified system where T_f in the transition rate (5) is set equal to zero if the spin $\vec{\sigma}_i$ to be updated belongs to the bulk, namely if it is aligned with all its neighbors. Since the bulk degrees of freedom, which alone contribute to $C_{st}(t-s)$, feel $T_f=0$, and $C_{st}(t-s) \equiv 0$ at $T_f=0$, by computing observables with this modified dynamics one isolates the aging term leaving other properties of the dynamics unchanged [15]. In order to check this we have computed $C(t,s)$ and $C_{st}(t-s)$ with the Glauber dynamics in a system with $p=3$ quenched to $T_f=1<T_1$ and in an equilibrium system at the same temperature. In Fig. 1 we compare $C_{ag}(t,s)$ obtained by subtraction of these quantities through Eq. (13) (symbols) and the same quantity obtained directly by means of a quench simulation with the modified dynamics (continuous lines). This figure shows an excellent agreement, confirming that the modified dynamics is efficient and accurate. In the remainder of this section therefore we will always present results obtained with this modified dynamics.

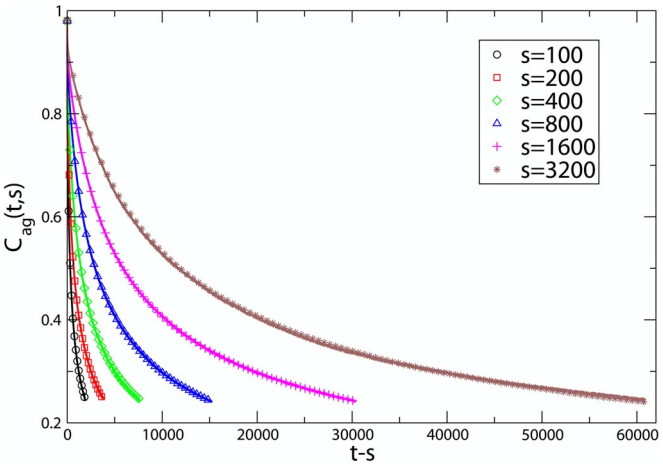

FIG. 1. (Color online) $C_{ag}(t,s)$ obtained with the two methods described in the text is plotted against $t-s$ for $s=100$, 200, 400, 800, 1600, 3200.

In the late stage of the evolution, after a characteristic time t_{sc} when $L(t)$ is much larger than all other microscopic lengths, dynamical scaling is obeyed [1,6]. Accordingly, for the correlation function one has

$$G_{ag}(r,t) = M^2 g(x), \tag{14}$$

where $x=r/L(t)$ and $\vec{M}$ is the equilibrium magnetization at T_f. In systems with a discrete symmetry and sharp interfaces, a short distance behavior ($x \ll 1$) of the type $1-g(x) \sim x$ is found [1,6], namely a Porod's tail $\hat{G}(\vec{k},t) \sim k^{-(d+1)}$, in momentum space for large k [$k \gg L(t)^{-1}$]. This is known to be true, in particular, for the clock model, for all $p<\infty$, although the whole form of $g(x)$ depends on p [6]. In systems with a vector order parameter and an $O(N)$ symmetry one has a generalization of the Porod's law [16], $\hat{G}(\vec{k},t) \sim k^{-(d+N)}$.

From Eq. (14) one can extract a quantity $L_1(t)$ proportional to the typical domain size $L(t)$ from the condition $g(x)=\frac{1}{2}$, namely as the half height width of $G_{ag}(r,t)$. Alter-

natively, a characteristic length $L_2(t)$ can be extracted as $L_2(t)=\int dr G_{ag}(r,t)$. Clearly, if Eq. (14) holds, $L_1(t) \propto L_2(t)$.

The size of domains can be related to the density of defects $\rho(t)$. For a coarsening system where topological defects are only interfaces, such as the Ising model, one has a power law behavior $\rho(t) \propto t^{-\delta}$, with [1]

$$\delta = 1/z. \tag{15}$$

This result does not apply to systems with different defects, such as vortices or others. In the case of vector $O(N)$ (with $N \geq 2$) model [1,17] one has

$$\delta = 2/z, \tag{16}$$

and logarithmic corrections for $N=2$. In these cases $\rho(t)$ provides an indirect, alternative method for the determination of $L(t)$, and hence of z. For the clock model, where defects are interfaces and vortices, neither Eq. (15) or Eq. (16) can be straightforwardly used. However, a simple inspection of the configurations (see Fig. 2) suggests that, since vortices are pointlike, their contribution to $\rho(t)$ must be negligible in the late stage. Therefore we expect Eq. (15) to be obeyed asymptotically.

The dynamical exponent z is believed to be universal for quenches to the ordered phase $T_f < T_1$: the same value $z=2$ as for the Ising model is expected for every value of p [5,6] in the clock model and for every N in $O(N)$ models.

Coming to two-times quantities, the aging part of the autocorrelation function is expected [1,14] to scale as

$$C_{ag}(t,s) = h(y), \tag{17}$$

with $y=t/s$ and $h(y) \sim y^{-\lambda/z}$ for $y \gg 1$. The exponent λ is believed to be the Fisher-Huse exponent which regulates the large t decay of the initial condition autocorrelation function $C(t,0) \sim t^{-\lambda/z}$. In the Ising model one has $\lambda = 5/4$. We are not aware of a systematic study of this exponent in the XY model. In Ref. [18] it is argued that this exponent depends on T_f and, for the particular case $T_f=0.3$ the value $\lambda=0.54$ is found. For the integrated response function scaling implies

$$\chi_{ag}(t,s) = s^{-a_\chi} f(y). \tag{18}$$

For $p=2$ the scaling function behaves as

$$f(y) \sim y^{-a_\chi}, \tag{19}$$

for $y \gg 1$. Regarding the exponent a_χ, analytical calculations in solvable scalar models or in the large-N model [19,20] find the following dependence on dimensionality:

$$a_\chi = \begin{cases} \delta \dfrac{d-d_L}{d_U-d_L} & \text{for } d < d_U \\ \delta \quad \text{with log corrections for } d = d_U \\ \delta \quad \text{for } d > d_U, \end{cases} \tag{20}$$

where d_L is the lower critical dimension of static critical phenomena and d_U is an upper dimension that turns out to be $d_U=3$ or $d_U=4$ for systems with a discrete or continuous symmetry. This expression shows that the response of coarsening systems depends on dimensionality in a nontrivial way. Numerical simulations [19,21,22] of scalar and $O(N)$ vectorial systems, with conserved and nonconserved order parameter, are consistent with Eq. (20). The value of a_χ is investigated for systems with a discrete symmetry and a degeneracy of the ground state larger than $p=2$.

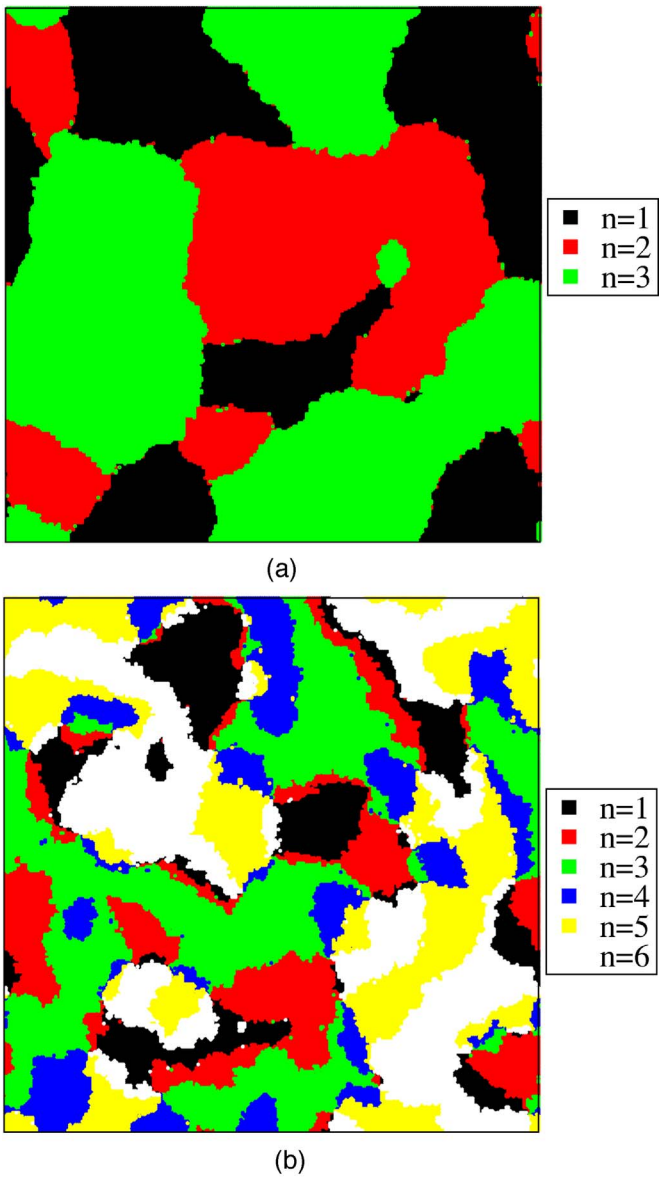

FIG. 2. (Color online) Configuration of the system with $p=3$ (left) and $p=6$ (right), at $t=3200$.

Notice that, for a given dimensionality $d < d_U$, Eq. (20) predicts a different exponent for systems with a continuous or a discrete symmetry. In the case $d=2$, for instance, for the Ising model Eq. (20) gives $a_\chi = 1/4$ while for the XY model $a_\chi = 0$. Therefore, for the model under investigation, the value of a_χ may be used to discriminate between the Ising and XY nonequilibrium universality classes.

Finally, let us recall that the scaling behaviors (14), (17), (18) are only expected asymptotically. Since numerical simulations can only access a finite time region, preasymptotic effects may be present. In particular in numerical simulations of the Ising model with a nonconserved order parameter, one usually observes an effective exponent $1/z_{eff} \simeq 0.48$ in place

of $1/z=0.5$. The integrated response function has been also shown [10,15] to be affected by corrections to scaling. These can be conveniently discussed in terms of the effective exponent, defined as

$$a_{eff}(y,s) = -\left.\frac{\partial \ln \chi_{ag}(t,s)}{\partial \ln s}\right|_y . \tag{21}$$

With a scaling form such as Eq. (18), one would have $a_{eff}(y,s)=a_\chi$, independent of y and s. However, if preasymptotic effects are present, the effective exponent takes a value which depends both on y and s. For $p=2$ it was shown [15] that, because of this, $a_{eff}(y,s)$ is found in numerical simulations in the range $0.25 \leq a_{eff}(y,s) \leq 0.28$.

B. Numerical results

In the following we will present the numerical results. Setting $J=1$, for each case considered we simulated a square lattice of size 1000^2 with periodic boundary conditions and an average over 100 realizations was performed. Statistical errors, when not explicitly plotted in the figures, are comparable to the thickness of the lines.

For $p=3$ there is a ferro-paramagnetic transition at $T_1 \simeq 1.326$ while for $p=6$, according to Eq. (4), one has $T_1 \simeq 0.645$. We performed a series of simulations of quenches to $T_f < T_1$, with $T_f=1/2$ or $T_f=1$ for $p=3$ and $p=6$, respectively. Typical configurations of domains in the late stage are shown in Fig. 2. Notice the simultaneous presence of interfaces and vortices. These are defined analogously to those of $O(N)$ models: on encircling a vortex the order parameter rotates by $\pm 2\pi$ (although in the clock model rotations are obtained by discrete steps). While for $p=3$ vortices and interfaces between different phases are all energetically equivalent, in the case $p=6$ one has the additional feature of different kinds of vortices and interfaces. Let us consider a domain characterized by having all the spins pointing along the direction $\theta=2\pi n/p$. Spins belonging to the domain are characterized by having the same value of n_i, $n_i=n$. This domain can be separated by an interface from another domain where spins point along a different direction $\theta=2\pi m/p$. Clearly, interfaces between domains of contiguous phases, namely with $n=m\pm 1$ are energetically less expensive then the others. The more energetically expensive interfaces are eliminated faster from the system (they are already practically absent in Fig. 2). This fact influences considerably the topology of the growing structure. For instance, one clearly observes that between two domains of noncontiguous phases, say with $n=m$ and $n=m+2$, a thin slab of phase $n=m+1$ is interposed in order to minimize energy.

Analogously one observes also different kinds of vortices. Points where six phases meet are energetically favored, but vortices where a lower number of phases meet can also be present. Moreover, there are also points where four (or more) domains meet, but two of them belong to the same phase: Encircling such points one may enter domains characterized respectively by, say, the sequence n, $n+1$, $n+2$, $n+1$ again. Clearly, encircling the most energetically favored vortices one finds all the phases according to the sequence n, $n+1$, $n+2$, $n+3$, $n+4$, $n+5$, $n+6$ (or in reverse order). As for the interfaces, the high energy vortices are quickly removed and a typical late stage configuration, as that of Fig. 2, contains practically only the lowest energy vortices. The presence of all these different kind of defects in the system is possibly the origin of the long lasting preasymptotic effects discussed below.

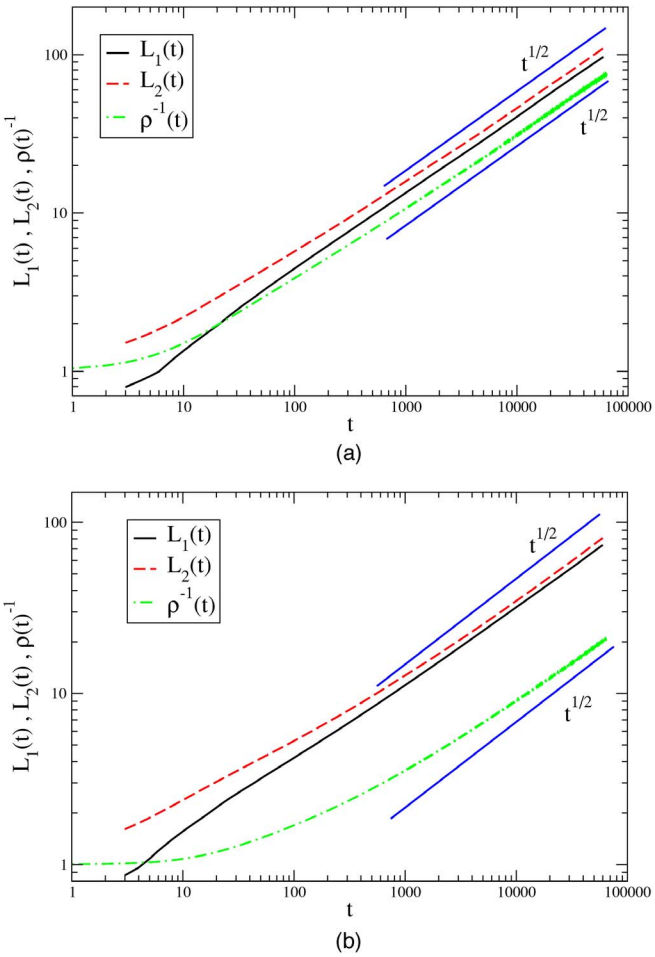

FIG. 3. (Color online) Comparison between $L_1(t)$, $L_2(t)$ and $\rho(t)^{-1}$ for $p=3$ (left) and $p=6$ (right).

A comparison between $L_1(t)$, $L_2(t)$, and $\rho(t)^{-1}$ is shown in Fig. 3. After an early stage when domains are formed and scaling does not hold, $L_1(t)$, $L_2(t)$, and $\rho(t)^{-1}$ start growing with an approximate power law behavior and for long times one has $L_1(t) \propto L_2(t) \propto \rho^{-1}(t)$ [for $p=6$, $\rho(t)^{-1}$ does not obey a power law behavior in the range of simulated times. However, for the longest simulated times the effective exponent seems to approach a value roughly comparable with that of $L_1(t)$ and $L_2(t)$]. This implies that Eq. (15) is obeyed asymptotically. We recall that for a system containing only vortices, such as the XY model, one would instead expect the relation (16). Regarding the coarsening exponent, in the decade 10^4–10^5 for $p=3$ we measure $1/z_{eff}=0.486\pm0.002$, $1/z_{eff}=0.484\pm0.002$, and $1/z_{eff}=0.478\pm0.002$ from $L_1(t)$, $L_2(t)$, and $\rho(t)^{-1}$, while for $p=6$ we get $1/z_{eff}=0.467\pm0.003$, $1/z_{eff}=0.474\pm0.003$, $1/z_{eff}=0.450\pm0.008$. These values (apart from the last one which is evidently a still preasymptotic effective exponent) are compatible with the value

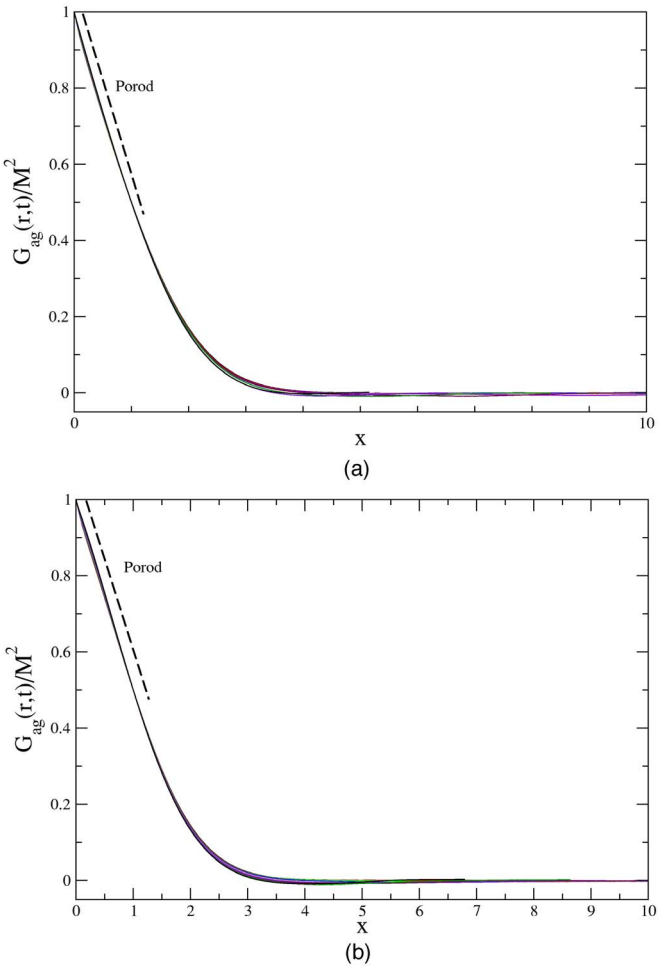

FIG. 4. (Color online) Data collapse of $G_{ag}(r,t)$ against $x=r/L_1(t)$ for several times t_n generated from $t_n=\mathrm{Int}[\exp(n/2)+1]$ with n ranging from 13 to 22 and $p=3$ (left) or $p=6$ (right).

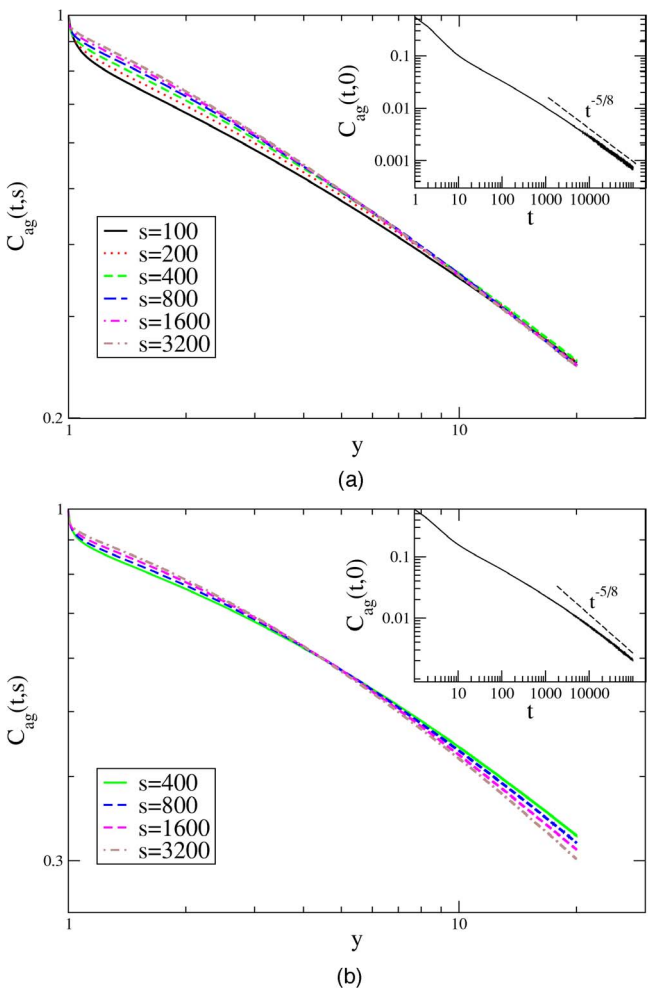

FIG. 5. (Color online) $C(t,s)$ is plotted against y for $p=3$ (left) with $s=100$, 200, 400, 800, 1600, 3200 and for $p=6$ (right) with $s=400$, 800, 1600, 3200. In the insets $C(t,0)$ is plotted against t.

$1/z=1/2$ of the Ising model. The different initial behaviors of $L_1(t)$, $L_2(t)$, and $\rho(t)^{-1}$, signal that preasymptotic effects are present up to very long times. This is probably related to the presence of different types of defects. Note also that, at the longest time considered, the density of defects with $p=6$ is more than three times larger than with $p=3$.

In Fig. 4 we test the scaling form (14) of the equal time correlation function. We plot $G_{ag}(r,t)/M^2$ against $x=r/L_1(t)$ for several values of t in the two decades range $[6.4\times10^2-6.4\times10^4]$. The data show a good collapse on a single master curve $g(x)$. For small x the Porod's behavior $1-g(x)\sim x$ is very neatly observed.

We turn now to consider two time quantities. In Fig. 5 the autocorrelation function is plotted against y for different values of s in the range $[100-3200]$. As already observed when discussing Fig. 3, scaling is only approximatively obeyed in this regime. This is mirrored by $C_{ag}(t,s)$: Full data collapse is not found. Regarding Fig. 3, we also noticed that scaling improves as time gets larger and it is reasonably well obeyed for the longest simulated times. The same conclusion can be drawn, for $p=3$, from $C_{ag}(t,s)$. Indeed, in Fig. 5 one can observe that the data collapse improves pushing s and y to larger values. In fact, although the data collapse of the curves is poor for small y it gets better increasing y and, for $y>10$, all the curves collapse. Moreover, the quality of the collapse improves also increasing s. Indeed, while the curves with small s do not collapse (except, as anticipated, for y as large as $y>10$) the two curves with the largest values of s ($s=1600$ and 3200) practically coincide for all $y>2$. For $p=6$ the collapse is worse. Coming to the asymptotic behavior of the scaling function $h(y)\sim y^{-\lambda/z}$, it is numerically too demanding to reach the asymptotic large-y region with the values of s considered in Fig. 5. Then, we have evaluated λ from the large t behavior of $C(t,0)$. This quantity is shown in the insets of Fig. 5. In the range $t\in[4\times10^4,10^5]$ we find $\lambda/z=0.61\pm0.01$ and $\lambda/z=0.57\pm0.01$ for $p=3$ and $p=6$. For $p=3$ this value is consistent with the value $\lambda/z=5/8=0.625$ of the Ising model, keeping also into account that the effective exponent we measure is still slightly increasing at the longest simulated times. For $p=6$ the measured exponent is somewhat smaller than for $p=3$ and for the Ising model, but the fact that it keeps still growing at the longest simulated times suggests that asymptotically the same value $\lambda=5/8=0.625$ could be obtained. This results suggest that there could be a unique nonequilibrium universality class for

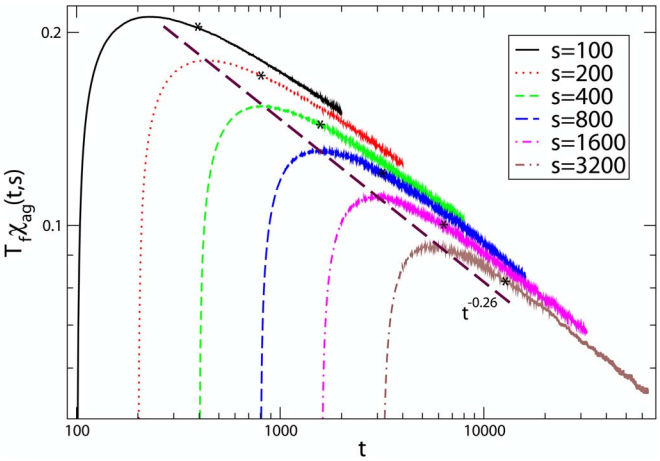

FIG. 6. (Color online) $T_f\chi_{ag}(t,s)$ is plotted against t for fixed values of s. The dashed line is the power law $t^{-0.26}$.

every $2 \leq p < \infty$. This hypothesis can be tested by considering the integrated response function. This quantity, for $p=3$, is plotted against t in Fig. 6, showing a marked dependence on s. Starting from zero at $t=s$, $\chi_{ag}(t,s)$ reaches a maximum at $t \simeq 2s$ and then decreases to zero with a power law behavior. A similar behavior is observed for $p=6$. According to Eq. (18), by fixing y to a certain value and varying s or equivalently t, the data should follow a power law with exponent $-a_\chi$. As an example, the points corresponding to $y=4$, which have been marked with stars in the log-log plot of Fig. 6, are approximatively aligned on a straight line of slope 0.26 ± 0.01. A similar analysis can be performed for every value of y.

In order to make a quantitative analysis of this exponent, and to detect preasymptotic effects, in Fig. 7 we plot $\chi_{ag}(t,s)$ for fixed values of y against s. According to Eq. (21) the slope of these lines is $a_{eff}(y,s)$ and, if scaling (18) holds, one should find $a_{eff}(y,s) \equiv a_\chi$. Preasymptotic effects, instead, introduce a weak dependence of this exponent on s and y. Apart from the curve $y=2$, which corresponds to very early times, the slopes of all the curves are compatible with Eq. (20), namely with $a_\chi = 1/4$ (for $p=3$ in the range $s \in [800-3200]$ we find $a_{eff}(y,s)=0.25-0.30$, depending on y. For $p=6$ the effect of preasymptoticity is smaller and one finds $a_{eff}(y,s) \leq 0.27$ for every value of y and s). This pattern of behavior of $a_{eff}(y,s)$ is similar to what is observed in the Ising model where $a_{eff}(y,s)$ ranges in the interval, $a_{eff}(y,s) = [0.25-0.28]$.

The data collapse of $s^{1/4}\chi_{ag}(t,s)$ vs y expected from Eq. (18) is shown in Fig. 8. For $p=6$ the collapse of the two curves with the largest s ($s=1600$, 3200), is good at sufficiently large y ($y>4$). It is poorer for $p=3$. Note also that the asymptotic behavior $f(y) \sim y^{-1/4}$ for $y \to \infty$ is well obeyed, consistently with Eq. (19), again confirming $a_\chi = 1/4$ and ruling out the value $a_\chi = 0$ appropriate to the XY model. These results strengthen the conclusion that the clock model below T_1 does not belong to the XY universality class and that the nonequilibrium universality class is the same for all $2 \leq p < \infty$.

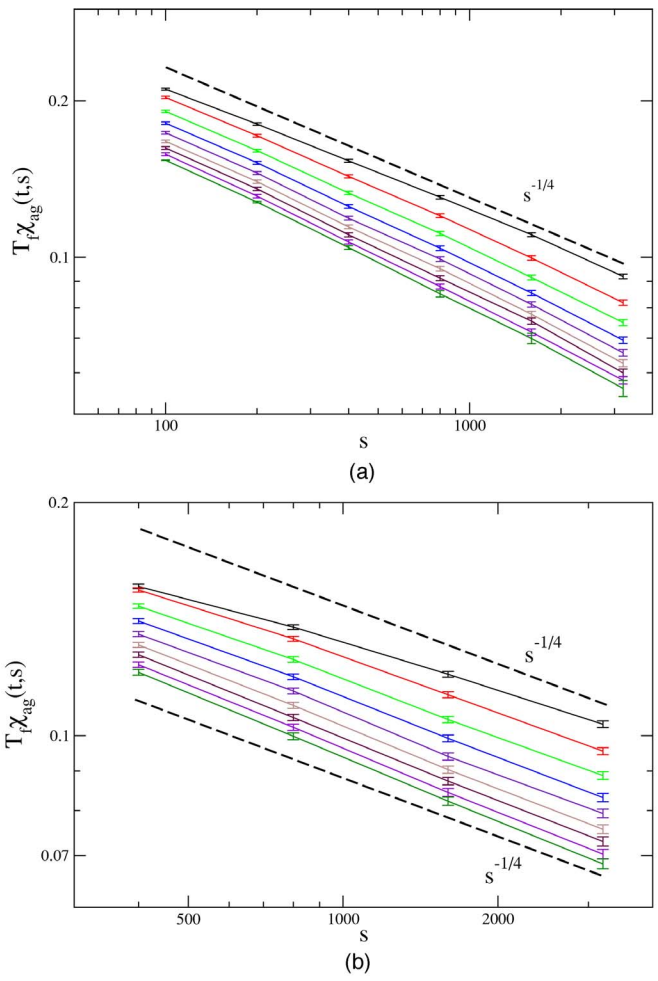

FIG. 7. (Color online) $T_f\chi_{ag}(t,s)$ is plotted against s for $p=3$ (left) and $p=6$ (right), with fixed values of y ($y=2$, 4, 6, 8, 10, 12, 14, 16, 18 from top to bottom). Numerical values are marked with error bars, continuous lines are guides for the eye.

IV. $p=6$: QUENCHES TO $T_1 \leq T_f \leq T_2$

Let us consider the model with $p=6$ quenched to the critical region $T_1 \leq T_f \leq T_2$. In the late stage the correlation function obeys Eq. (2). From this equation one has

$$I(t) = \int dr G(r,t) \propto L(t)^{3-d-\eta} \sim t^{(3-d-\eta)/z}. \tag{22}$$

$L(t)$ can then be extracted as

$$L(t) \propto I(t)^{1/(3-d-\eta)}. \tag{23}$$

The autocorrelation function obeys [14,23]

$$C(t,s) = (t-s+t_0)^{-(d-2+\eta)/z} \tilde{h}(y), \tag{24}$$

where t_0 is a microscopic time. Neglecting t_0 for $t-s \gg t_0$, $C(t,s)$ can be rewritten in scaling form

$$C(t,s) \simeq s^{-(d-2+\eta)/z} h(y), \tag{25}$$

where $h(y) = (y-1)^{-(d-2+\eta)/z} \tilde{h}(y)$, with the property $h(y) \sim y^{-\lambda/z}$ for $y \gg 1$. Notice that, when using the y variable in

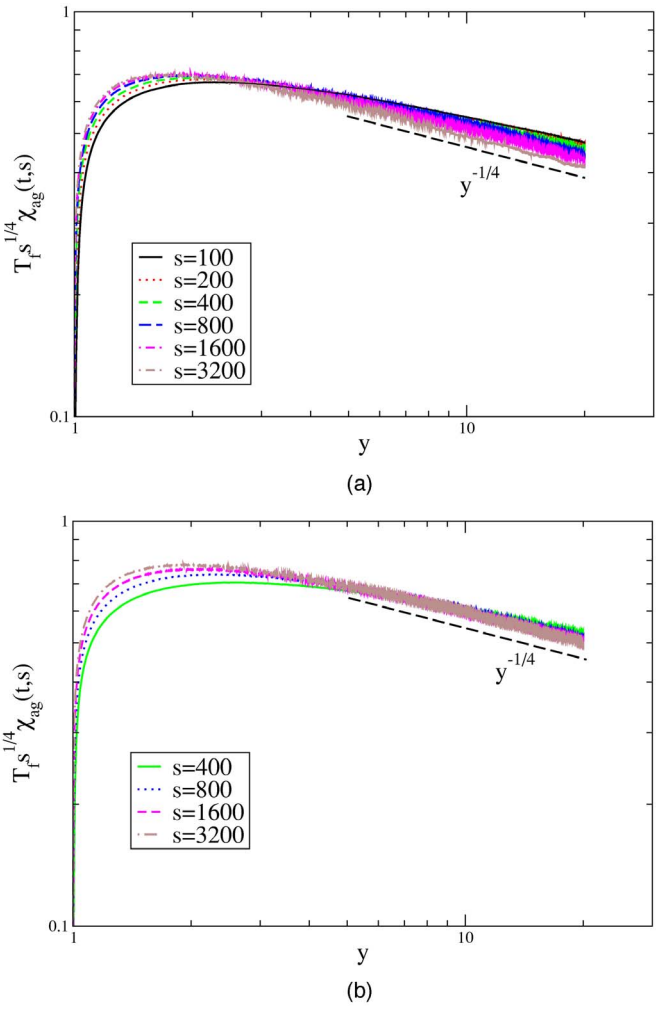

FIG. 8. (Color online) $T_f s^{1/4} \chi_{ag}(t,s)$ is plotted against y for fixed values of s for $p=3$ (left) and $p=6$ (right).

the large-s limit, the condition $t-s \gg t_0$ for the validity of Eq. (25) becomes $y>1$. For all $y>1$, then, one should expect data collapse of the curves $s^{(d-2+\eta)/z} C(t,s)$ against y for different choices of s.

The response function is given by [14,23]

$$R(t,t') = (t - t' + t_0)^{-(d-3+\eta)/z} \tilde{f}\left(\frac{t'}{t}\right). \tag{26}$$

Splitting the integral of Eq. (9) into two integration domains, introducing the arbitrary number ϵ, the integrated response function can be written as

$$\chi(t,s) \sim t^{-(d-2+\eta)/z} \left[\int_y^{1-\epsilon} du \left(1 - u + \frac{t_0}{t}\right)^{-(d-3+\eta)/z} \tilde{f}(u) + \int_{1-\epsilon}^{1} du \left(1 - u + \frac{t_0}{t}\right)^{-(d-3+\eta)/z} \tilde{f}(u) \right] \tag{27}$$

$$= t^{-(d-2+\eta)/z} \left[I_1\left(y, \frac{t_0}{t}, \epsilon\right) + I_2\left(\frac{t_0}{t}, \epsilon\right) \right], \tag{28}$$

where $u=t'/t$. For large times t one can choose $t_0/t \ll \epsilon \ll 1/2$. The condition $t_0/t \ll \epsilon$ allows one to neglect t_0/t with respect to $1-u$ in the first integral, whose value can then be evaluated as $I_1(y,t_0/t,\epsilon) \simeq F(1-\epsilon,t_0/t) - F(y,0)$, where $dF(u,t_0/t)/du = \left(1-u+\frac{t_0}{t}\right)^{-(d-3+\eta)/z} \tilde{f}(u)$. Let us consider now the second integral $I_2(t_0/t,\epsilon) = F(1,t_0/t) - F(1-\epsilon,t_0/t)$. Here, since $\epsilon \ll 1/2$, one can set $\tilde{f}(u) \simeq f(1)$, so that $F(1,t_0/t) \simeq (t_0/t)^{-(d-2+\eta)/z} \tilde{f}(1) z/(d-2+\eta)$. One then arrives at

$$\chi(t,s) = t^{-(d-2+\eta)/z} f(y) + \frac{\tilde{f}(1)}{(d-2+\eta)/z} t_0^{-d-2+\eta/z}, \tag{29}$$

where $f(y) = -F(y,0)$. Letting $t \to \infty$, $\chi(t,s)$ must converge to the equilibrium susceptibility whose value is given by the fluctuation dissipation theorem, $\chi_{eq} = T_f^{-1}$. This leads to the identification of the last term on the right-hand side of Eq. (29) with χ_{eq} [24], and Eq. (29) can be cast as

$$\chi(t,s) - \chi_{eq} \sim s^{-a_\chi} f(y), \tag{30}$$

where $a_\chi = (d-2+\eta)/z$. Notice that, differently from the case of quenches in the ordered phase, here the exponent a_χ is directly related to the equilibrium critical exponents η and z. We recall that, in the KT phase, the exponents η, z, λ depend on temperature.

It is interesting to discuss the parametric plot of $\chi(t,s)$ against $C(t,s)$. Since $C(t,s)$ is a monotonically decreasing function of t, this time can be re-parametrized in terms of C, obtaining $\chi(t,s) = \hat{\chi}(C,s)$. This quantity is important because, if appropriate conditions are satisfied, its large-s limit

$$\hat{\chi}(C) = \lim_{s \to \infty} \hat{\chi}(C,s) \tag{31}$$

provides a connection between static and dynamic properties [25,26] through the relation

$$P(q) = -T_f \left. \frac{d^2 \hat{\chi}(C)}{dC^2} \right|_{C=q}, \tag{32}$$

where $P(q)$ is the overlap probability function of the equilibrium state at $T=T_f$. As discussed in Ref. [14], a universal linear relation

$$T_f \hat{\chi}(C) = T_f \chi_{eq} - C, \tag{33}$$

as for equilibrated systems, is expected for quenches to a critical point or into a critical phase, although the system is aging for any finite time.

Numerical results

In this section we present results of simulations of the model with $p=6$ quenched to $T_1 < T_f = 0.76 < T_2$. A typical configuration of domains in the late stage is shown in Fig. 9. In this case, there are no compact domains.

The quantity $I(t)$ is shown in Fig. 10. Here one observes that the power law behavior sets in very early. This implies, through Eq. (22), that also $L(t)$ has a power law growth. The effective exponent has a small tendency to increase as t gets

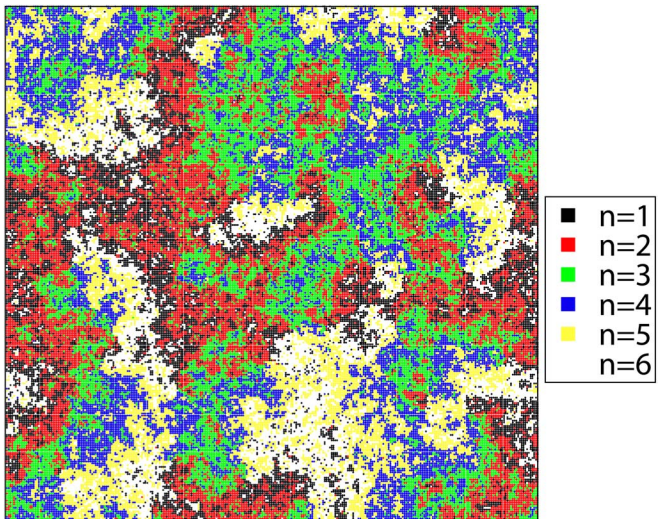

FIG. 9. (Color online) Configuration of the system at $t=3200$ after a quench to $T_f=0.76$.

larger: We measure an exponent 0.34 in the decade 10^2-10^3 and 0.35 for $t>10^4$. The exponents η and z are known numerically [9]. At $T_f=0.76$ their measure gives $\eta=0.17$ and $z=2.18$, yielding $(3-d-\eta)/z=0.38$. This number is consistent with the value 0.35 obtained from $I(t)$ by means of Eqs. (23), taking also into account that the effective exponent we measure is still increasing at the longest simulated times.

In Fig. 11 we test the scaling form (2) of the equal time correlation function. We plot $r^{\eta}G_{ag}(r,t)$ against x for several values of t, where $L(t)$ is computed through Eq. (23). The data show a very good collapse on a single master curve $g(x)$. Notice that, as expected, Porod's behavior at small x is not observed, due to the noncompact nature of the domains.

We turn now to consider two time quantities. In Fig. 12 the autocorrelation function is shown. There is a tendency to a better data collapse for larger times, implying that the scaling symmetry is still not exactly obeyed. For the two largest values $s=50$ and $s=100$, however, the collapse is rather good.

Let us consider the integrated response function, that is shown in Fig. 13. Here one observes an analogous situation:

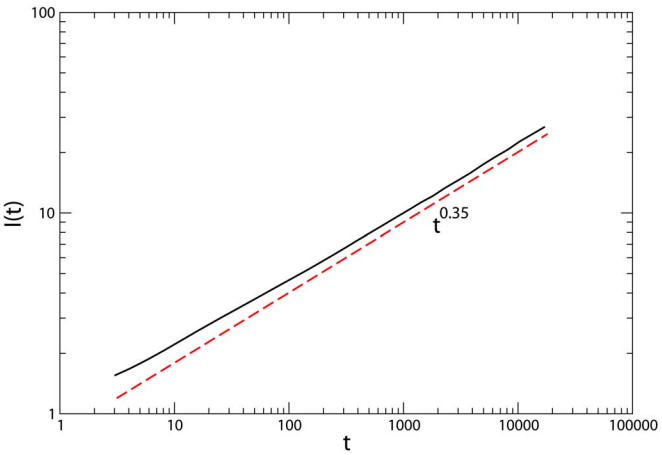

FIG. 10. (Color online) The behavior of $I(t)$. The dashed line is the power law $t^{0.35}$.

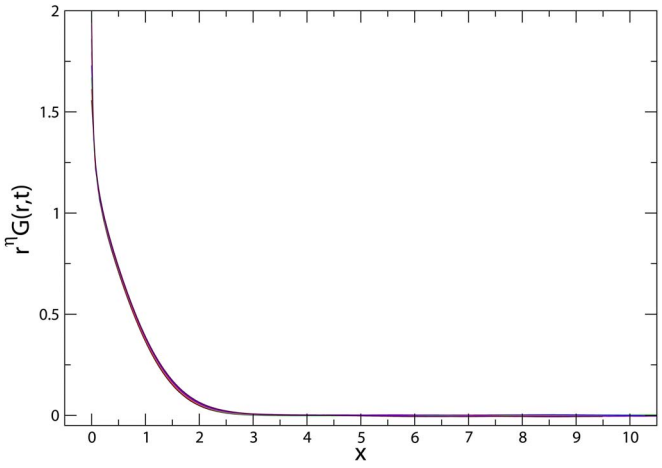

FIG. 11. (Color online) Data collapse of $r^{\eta}G(r,t)$ against x for several times (t=666, 1097, 1809, 2981, 4915, 8104, 13 360, 17 155).

the collapse expected on the basis of Eq. (30) is rather good for the two largest values of s.

In Fig. 14 the parametric plot of $\hat{\chi}(C,s)$ is shown. For the largest values of C, $\hat{\chi}(C,s)$ obeys Eq. (33). As C is decreased the curves flatten and $T_f\hat{\chi}(C,s)$ lies below the asymptotic curve (33). However, in the limit of infinite times $t\to\infty$, which corresponds to $C\to 0$, each curve must necessarily obey Eq. (33), since $\chi(t,s)$ approaches the equilibrium value $\chi_{eq}=1/T_f$. Then, moving toward $C=0$, at some point the curves become steeper in order to meet the value χ_{eq} at $C=0$. Changing s, the same qualitative behavior is observed, but the curve gets higher, slowly approaching the asymptotic form (33) for all values of C in the large s limit. This pattern of $\hat{\chi}(C,s)$ is analogous to what observed in the spherical model quenched at the critical point and is expected in full generality whenever a system is quenched to a critical point or to a critical phase [14]. It must be noticed that the convergence to the trivial form (33) is very slow because it is regulated by the rather small exponent $\eta(T)$ [14]. Since the exponent $\eta(T)$ at the lower transition temperature is expected to behave as $\eta(T_1)\simeq 4/p^2$, the asymptotic behavior can be

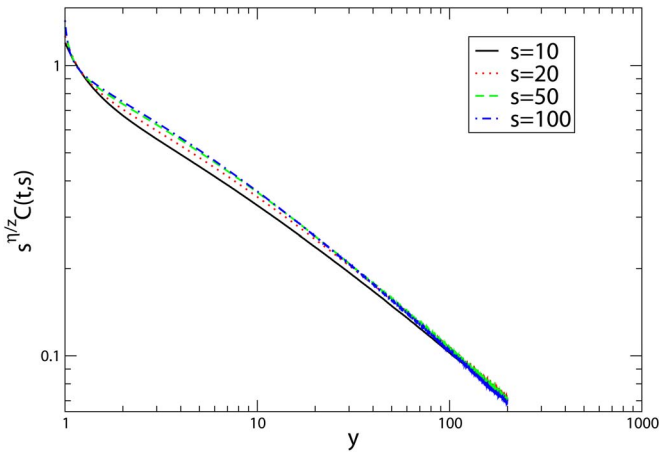

FIG. 12. (Color online) Data collapse of $C(t,s)$, for $s=10$, 20, 50, 100 (from bottom to top).

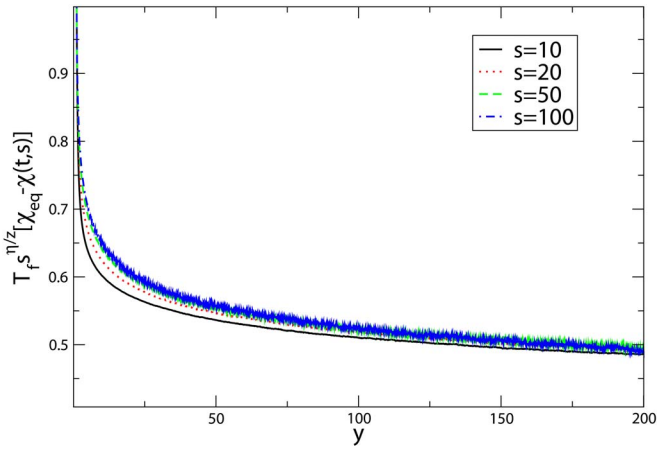

FIG. 13. (Color online) Data collapse of $\chi(t,s)$ in the quench at $T_f=0.76$, for $s=10$, 20, 50, 100 (bottom up).

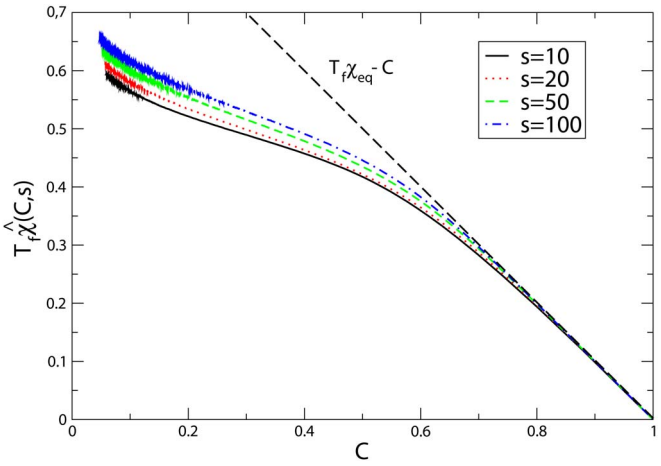

FIG. 14. (Color online) Parametric plot of $\chi(t,s)$ vs $C(t,s)$ in the quench at $T_f=0.76$, for $s=10$, 20, 50, 100 (bottom up). The dashed line is the asymptotic curve $T_f\chi(C)=T_f\chi_{eq}-C$, Eq. (33).

arbitrarily delayed increasing p. The simulations presented in this section have been planned out in order to show at least a glimpse of this convergence. As discussed in Ref. [14], previous studies of the KT phase of the XY model, for which the same asymptotic form (33) is expected, interpreted a preasymptotic nontrivial form of $\hat{\chi}(C,s)$ analogous to the one of Fig. 14 as a reminiscence of the parametric plot of the $d=3$ Edwards-Anderson model [18] or used it to infer the asymptotic value of the fluctuation-dissipation ratio [27]. The simulations presented here clearly show, instead, that this pattern is preasymptotic and the data are consistent with a convergence to the expected trivial limiting form (33).

V. CONCLUSIONS

In this paper a rather general numerical investigation of the off-equilibrium dynamics of the clock model after a temperature quench has been carried out. We have considered both quenches into the ordered phase $T_f<T_1$ for systems with $p=3$ and $p=6$ and a quench to the critical, Kosterlitz-Thouless phase $T_1<T_f<T_2$, for $p=6$. In all these cases we analyzed the behavior of one-time quantities, such as the equal time correlation function or the characteristic length, and two-times quantities, such as the integrated response and the autocorrelation function. This study provides a quite general scenario of the scaling properties of the dynamics and allows the comparison with the behavior of other well studied coarsening systems such as the Ising model or the XY model, which correspond to the case $p=2$ and $p=\infty$, respectively. We find that dynamical scaling is obeyed in all the cases considered. In the ordered region, the dynamical exponents are the same of those of the Ising model. While the result $z=2$ for the clock model was already well known [5,6] the values of the exponents λ and a_χ have been measured for the first time and deserve some considerations. These values suggest that the clock model belongs to the nonequilibrium universality class of the Ising model. Moreover, finding the same values of the exponents for both $p=3$ and $p=6$ implies that the system is in the same equilibrium universality class for all $p<\infty$. Finally, the value $a_\chi=1/4$ fits with the general phenomenological formula (20) for coarsening systems. This strengthens the idea that the nontrivial dimensionality dependence of a_χ predicted by Eq. (20), may have a general validity for coarsening dynamics.

It has been recently proposed [22,28] that, limited to the case of systems where topological defects are exclusively domain walls, Eq. (20) may be related to the dynamical roughening of the interfaces. The fact that the value of a_χ is the same also in the clock model implies that the asymptotic contribution of vortices to the response function is not important, at least at the level of the exponent a_χ, and suggests that the behavior of the interfaces is the unifying feature that makes systems with different degeneracy p fall into the same universality class.

ACKNOWLEDGMENT

This work has been partially supported from MURST through Grant No. PRIN-2004.

[1] A. J. Bray, Adv. Phys. **43**, 357 (1994).
[2] P. C. Hohenberg and B. I. Halperin, Rev. Mod. Phys. **49**, 435 (1977).
[3] C. Chatelain, J. Stat. Mech.: Theory Exp. 2004, P06006.
[4] G. Odor, Rev. Mod. Phys. **76**, 663 (2004).
[5] K. Kaski and J. D. Gunton, Phys. Rev. B **28**, 5371 (1983).
[6] F. Liu and G. F. Mazenko, Phys. Rev. B **47**, 2866 (1993).
[7] J. V. José, L. P. Kadanoff, S. Kirkpatrick, and D. R. Nelson, Phys. Rev. B **16**, 1217 (1977); D. A. Nelson, in *Phase Transitions and Critical Phenomena*, edited by Domb and J. L. Lebowitz (Academic Press, London, 1983).
[8] J. M. Kosterlitz and D. J. Thouless, J. Phys. C **6**, 1181 (1973);

J. M. Kosterlitz, *ibid.* **7**, 1046 (1974).
[9] M. S. S. Challa and D. P. Landau, Phys. Rev. B **33**, 437 (1986); P. Czerner and U. Ritschel, Phys. Rev. E **53**, 3333 (1996).
[10] C. Chatelain, J. Phys. A **36**, 10739 (2003).
[11] F. Ricci-Tersenghi, Phys. Rev. E **68**, 065104(R) (2003).
[12] E. Lippiello, F. Corberi, and M. Zannetti, Phys. Rev. E **71**, 036104 (2005).
[13] In Ref. [12] the relation (11) was derived making explicit reference for simplicity to scalar spins $\sigma_i = \pm 1$. However, the same derivation applies as well to vector spins.
[14] F. Corberi, E. Lippiello, and M. Zannetti, J. Stat. Mech.: Theory Exp. 2004, P12007.
[15] F. Corberi, E. Lippiello, and M. Zannetti, Phys. Rev. E **72**, 056103 (2005).
[16] M. Mondello and N. Goldenfeld, Phys. Rev. A **42**, 5865 (1990); **45**, 657 (1992); A. J. Bray and S. Puri, Phys. Rev. Lett. **67**, 2670 (1991); F. Liu and G. F. Mazenko, Phys. Rev. B **45**, 6989 (1992); **46**, 5963 (1992); H. Toyoki, *ibid.* **45**, 1965 (1992); A. J. Bray and K. Humayun, J. Phys. A **25**, 2191 (1992).
[17] R. E. Blundell and A. J. Bray, Phys. Rev. E **49**, 4925 (1994).
[18] L. Berthier, P. C. W. Holdsworth, and M. Sellitto, J. Phys. A **34**, 1805 (2001).
[19] F. Corberi, E. Lippiello, and M. Zannetti, Phys. Rev. E **63**, 061506 (2001); Eur. Phys. J. B **24**, 359 (2001).
[20] F. Corberi, E. Lippiello, and M. Zannetti, Phys. Rev. E **65**, 046136 (2002).
[21] F. Corberi, E. Lippiello, and M. Zannetti, Phys. Rev. Lett. **90**, 099601 (2003); Phys. Rev. E **68**, 046131 (2003).
[22] F. Corberi, C. Castellano, E. Lippiello, and M. Zannetti, Phys. Rev. E **70**, 017103 (2004).
[23] H. K. Janssen, B. Schaub, and B. Schmittmann, Z. Phys. B: Condens. Matter **73**, 539 (1989); C. Godrèche and J. M. Luck, J. Phys.: Condens. Matter **14**, 1589 (2002); P. Calabrese and A. Gambassi, J. Phys. A **38**, R133 (2005).
[24] This result can be checked directly. In order to do this it is sufficient to observe that, due to local equilibrium, the fluctuation dissipation theorem must be obeyed also out of equilibrium for short time separations. Namely, by defining $X(t,s) = T_f R(t,s)/[\partial C(t,s)/\partial s]$, for $t \simeq s$ one must have $X(t,s)=1$. In this regime, using Eqs. (24) and (26) one has $X(t,s) = T_f \tilde{f}(1)/[(d-2+\eta)\tilde{h}(1)/z - (t-s+t_0)h'(1)/s]$, where $h'(y) = dh/dy$. For large s the last term in the denominator can be neglected. Since $C(t,t) \equiv 1$, from Eq. (24) one obtains $t_0^{-(d-2+\eta)/z}\tilde{h}(1)=1$. Using this expression to eliminate $\tilde{h}(1)$ in $X(t,s)$ gives $X(t,s) = T_f \tilde{f}(1) t_0^{-(d-2+\eta)/z} z/(d-2+\eta)$. The condition $X(t,s)=1$ for $t \simeq s$ leads then to the result anticipated in Sec. IV, namely $\tilde{f}(1) z t_0^{-(d-2+\eta)/z}/(d-2+\eta) = \frac{1}{T_f} = \chi_{eq}$.
[25] A. Barrat, Phys. Rev. E **57**, 3629 (1998).
[26] S. Franz, M. Mézard, G. Parisi, and L. Peliti, Phys. Rev. Lett. **81**, 1758 (1998); J. Stat. Phys. **97**, 459 (1999).
[27] S. Abriet and D. Karevski, Eur. Phys. J. B **37**, 47 (2004).
[28] M. Henkel, M. Paessens, and M. Pleimling, Phys. Rev. E **69**, 056109 (2004).